Europe PMC Funders Group
Author Manuscript
Biochem Pharmacol. Author manuscript; available in PMC 2020 May 18.

Published in final edited form as:
Biochem Pharmacol. 2019 June 01; 164: 34–44. doi:10.1016/j.bcp.2019.03.024.

The osteogenic effect of liraglutide involves enhanced mitochondrial biogenesis in osteoblasts

Subhashis Pal[a], **Shailendra K. Maurya**[a], **Sourav Chattopadhyay**[b], **Shyamsundar Pal China**[a], **Konica Porwal**[a], **Chirag Kulkarni**[a,d], **Sabyasachi Sanyal**[b], **Rohit A. Sinha**[c], **Naibedya Chattopadhyay**[a,d,*]

[a]Division of Endocrinology and Center for Research in Anabolic Skeletal Target in Health and Illness (ASTHI), Central Drug Research Institute (CDRI), Council of Scientific and Industrial Research (CSIR), Lucknow 226031, India

[b]Division of Biochemistry, Central Drug Research Institute (CDRI), Council of Scientific and Industrial Research (CSIR), Lucknow 226031, India

[c]Department of Endocrinology, Sanjay Gandhi Postgraduate Institute of Medical Sciences, Lucknow 226014, India

[d]AcSIR, CSIR-Central Drug Research Institute Campus, Lucknow 226031, India

Abstract

Liraglutide (Lira), a long-acting glucagon-like peptide 1 receptor (GLP1R) agonist reduces glycosylated hemoglobin in type 2 diabetes mellitus patients. Lira is reported to have bone conserving effect in ovariectomized (OVX) rats. Here, we investigated the osteoanabolic effect of Lira and studied the underlying mechanism. In established osteopenic OVX rats, Lira completely restored bone mass and strength comparable to parathyroid hormone (PTH 1-34). Body mass index normalized bone mineral density of Lira was higher than PTH. The serum levels of osteogenic surrogate pro-collagen type 1 N-terminal pro-peptide (P1NP) and surface referent bone formation parameters were comparable between Lira and PTH. GLP1R, adiponectin receptor 1 (AdipoR1) and peroxisome proliferator-activated receptor gamma coactivator 1-alpha (PGC1α) levels in bones were down-regulated in the OVX group but restored in the Lira group whereas PTH had no effect. In cultured osteoblasts, Lira time-dependently increased GLP1R, AdipoR1 and PGC1α expression. In osteoblasts, Lira rapidly phosphorylated AMP-dependent protein kinase (AMPK), the cellular energy sensor. Exendin 3, a selective GLP1R antagonist and PKA inhibitor H89 blocked Lira-induced increases in osteoblast differentiation, and expression levels of AdipoR1 and PGC1α. Furthermore, H89 inhibited Lira-induced phosphorylation of AMPK and dorsomorphin, an AMPK inhibitor blocked the Lira-induced increases in osteoblast differentiation and AdipoR1 and PGC1α levels. Lira increased mitochondrial number, respiratory proteins and respiration in osteoblasts *in vitro* and *in vivo*, and blocking mitochondrial respiration mitigated

*Corresponding author. n_chattopadhyay@cdri.res.in (N. Chattopadhyay).

Disclosures

Subhashis Pal, Shailendra K. Maurya, Sourav Chattopadhyay, Shyamsundar Pal China, Konica Porwal, Chirag Kulkarni, Sabyasachi Sanyal, Rohit Sinha, Naibedya Chattopadhyay declare that they have no conflict of interest.

Europe PMC Funders Author Manuscripts
Europe PMC Funders Author Manuscripts

Lira-induced osteoblast differentiation. Taken together, our data show that Lira has a strong osteoanabolic effect which involves upregulation of mitochondrial function.

Keywords

Osteoanabolic; Bone strength; Adiponectin receptor; Mitochondrial biogenesis; Glucagon-like peptide

1 Introduction

Incretins stimulate insulin secretion from pancreatic β-cells in a glucose-dependent manner and suppress glucagon secretion. Two most common incretins are glucagon like peptide-1 (GLP-1) and glucose-dependent insulinotropic polypeptide (GIP). Secreted from intestinal L-cells, GLP-1 binds with GLP-1 receptor (GLP1R) on pancreatic β-cells to maintain glucose homeostasis. Endogenous GLP-1 has a very short half-life (barely 5 mins) due to degradation by the ubiquitous protease dipeptidyl peptidase 4 (DPP-4) which precluded its use in diabetes therapy. Therefore, long-acting GLP-1 analogs having high structural homology with human GLP-1 and resistance to DPP-4 cleavage were designed to prolong its half-life. Approved drugs in this class of GLP1R agonists include exendin-4, albiglutide, lixisenatide and liraglutide (Lira). At a dose much higher than that required for glycemic control in patients with type 2 diabetes, Lira was shown to cause weight loss in obese individuals without type 2 diabetes mellitus [1], and is currently in use for the treatment of obesity, which suggests its potential use in non-diabetic individuals with other pathologies such as osteoporosis.

GLP-1 and exendin-4 have been shown to decrease hyperlipidemia-induced bone loss [2] and the later promoted bone formation in an insulin-resistant rat model [3], which suggested the skeletal effect of GLP1R agonists in diseases of glucose and energy metabolism. Subsequently, in ovariectomized (OVX) animals (preclinical model of postmenopausal osteopenia), both Lira and exendin-4 preserved bone mass likely via the GLP1R's indirect anti-resorptive effect (given its absence in osteoclasts) mediated by increased production of the anti-osteoclastogenic hormone, calcitonin [4,5]. GLP1R is functionally expressed in cultured bone marrow-derived osteoblastic cells and promotes their differentiation [6]. However, concerning the osteoanabolic effect, i.e. *de novo* bone formation, reports with GLP1R agonists are not definitive.

Mitochondrial malfunction is responsible for both insulin resistance and pancreatic β-cell dysfunction, resulting in glucose intolerance and type 2 diabetes mellitus [7]. In β -cells, reduced ATP generation due to impaired mitochondrial oxidative phosphorylation (OxPhos) appears to lower the closure of the ATP-sensitive K^+ channel which is necessary for insulin secretion. In skeletal muscle, reduced mitochondrial fatty acid oxidation leads to higher levels of long-chain acyl CoA and diacylglycerol which increases phosphorylation of insulin receptor substrate-1 thereby giving rise to insulin resistance [8]. Activating GLP1R has been shown to increase mitochondrial biogenesis in both β-cells and skeletal muscle resulting in increased insulin production and improving glucose tolerance [9]. Furthermore, GLP1R activation has been shown to promote mitochondrial biogenesis in white adipocytes thereby

Europe PMC Funders Author Manuscripts

Europe PMC Funders Author Manuscripts

converting them to brown adipocytes that are more efficient in energy expenditure via enhanced OxPhos [10].

Osteoblast differentiation is an energy demanding process as at this stage high amounts of collagen are synthesized and secreted. Whether glycolysis or OxPhos is used to meet the energy demand of differentiating osteoblasts remains uncertain. Guntur et al have shown that both glycolysis and OxPhos are increased in mouse calvarial osteoblasts to produce calcified nodules [10]. Esen et al have shown that the osteogenic drug teriparatide (human PTH 1-34) stimulates aerobic glycolysis in an insulin-like growth factor-1-dependent mechanism [11]. Activation of the osteoanabolic wnt pathway promotes osteogenesis by glutaminolysis and OxPhos [12]. We have recently shown that globular adiponectin promotes OxPhos in osteoblasts to promote bone formation [13]. Given the profound effect of GLP1R in the body's energy metabolism, we speculated that this receptor would modulate osteoblast function by regulating cellular bioenergetics.

In a longitudinally designed study, we tested whether Lira could restore established osteopenia in rats by *de novo* bone formation, and compared the skeletal response with parenterally administered human PTH 1-34 (the osteoanabolic drug). We also studied bioenergetics regulation of osteoblast function downstream of GLP1R activation by Lira.

2 Materials and methods

2.1 Reagents and chemicals

All the chemicals were purchased from Sigma-Aldrich (St. Louis, MO, USA) unless stated otherwise. Liraglutide was purchased from Novo Nordisk (Bagsvaerd, Denmark) and human PTH (1-34) was purchased from calbiochem (Kenilworth, NJ, USA). ELISA kits for rat procollagen type 1 N-terminal peptide (P1NP) was from My BioSource Inc. (San Diego, CA, USA). GLP1R inhibitor exendin 3 (Cat no 2081), protein kinase A inhibitor H89 (Cat no 2910) and AMPK inhibitor dorsomorphin (compound C) (Cat no 3093) were purchased from Tocris (Bristol, United Kingdom).

2.2 In vivo studies

Female Sprague Dawley (SD) rats were obtained from the National Laboratory Animal Centre, CSIR-CDRI. Animal care and experimental procedures were approved by the Institutional Animal Ethics Committee (IAEC, approval # CDRI/IAEC/2014/146). Animals were caged and maintained at 22–25 °C with a 12 h light/dark cycle. During the experimental period, the rats were maintained on standard rodent chow diet and purified water available ad libitum. Before surgery animals were anaesthetized using xylazine (10 mg/kg) and ketamine (40 mg/kg) injection (intramuscular).

2.2.1 Fracture healing—For experiments on fracture healing, 30 SD rats (200 ± 20 g) were divided into 3 groups and drill-holes were made by using a drill bit of 0.8 mm at femoral mid-diaphysis according to our previously published protocol [14]. One day after surgery, animals were divided into three equal groups; one group received vehicle (water), other two received Lira (0.3- or 0.6 mg/kg s.c.) for 12 days.

Europe PMC Funders Author Manuscripts
Europe PMC Funders Author Manuscripts

Europe PMC Funders Author Manuscripts

Europe PMC Funders Author Manuscripts

For studies in OVX rats, 20 adult female SD rats (250 ± 30 g, 8–10 months) underwent bilateral OVX. All animals were left untreated for osteopenia to develop which was confirmed by live animal μCT scan after 12 weeks. After confirming significant femoral bone loss, drill-hole was made as described above. 0.3 mg/kg Lira was administered subcutaneously for 12 days.

Calcein (20 mg/kg) was injected 24 h before sacrificing each animal to measure new bone formation at the drill-hole site. After the autopsy, all bones were frozen at −20 °C for μCT and microscopic analyses [15].

Bones were cleaned to remove soft tissue and were embedded in acrylic material. 50 μm sections through the drill-hole were prepared using Isomet-slow speed bone cutter (Buehler, Lake Bluff, IL) followed by confocal microscopy (Carl Zeiss LSM 510 meta confocal microscope, Zeiss Germany) to determine calcein intensity.

2.2.2 Reversal of osteopenia—40 adult female SD rats (250 ± 30 g, 8–10 months) underwent either sham surgery or ovariectomy (OVX). 12 weeks post-surgery, rats were scanned using μCT to ensure the development of osteopenia [15]. After successful development of osteopenia, rats were divided into the following groups (n = 10/group), sham + vehicle (water), OVX + vehicle, OVX + Lira (0.3 mg/kg; s.c.), OVX + PTH 1–34 (40 μg/kg; s.c.). Treatments were given for 12 weeks. Bones (tibia, femur, and fifth lumbar vertebra) and serum samples were collected after the treatment period and stored at −80 °C until further analysis. Calcein (20 mg/kg i.p.) was administered to each rat at an interval of 10 days before sacrifice for dynamic histomorphometry.

2.2.3 Analyses of bones—μCT (2D and 3D) assessment of live rats and isolated bones thereof was performed using a Sky Scan 1076 μCT scanner (SkyScan, Ltd, Kartuizersweg, Kontich, Belgium) as described before [16]. For volumetric BMD (vBMD), hydroxyapatite phantom rods of 4 mm of diameter with known BMD (0.25 g/cm^3 and 0.75 g/cm^3) was used for calibration as described before [15].

Body Mass Index (BMI) was calculated by using the formula BMI = Body weight/height^2. The height of each animal was determined by measuring snout to tail length. Bone mineral content (BMC) was calculated by using the formula BMC = BMD X bone volume (BV).

Biomechanical strength was assessed by compression test of the fifth lumbar vertebra (L5) using a bone strength tester (TK-252C; Muromachi Kikai, Tokyo, Japan) as described before [17]. L5 was placed on a stage of bone strength tester for compressive strength measured by pressure at a speed of 2.5 mm/min. From the load-displacement curve, the stiffness (N/mm), ultimate load (N), and energy to failure (mJ) were determined. Regression analysis at L5 vertebrae was performed by using GraphPad Prism 5 to determine a correlation between peak load (N) and bone mineral content (BMC).

For the determination of dynamic bone formation, bones were fixed at 70% ethanol and then methyl methacrylate blocks were prepared as per previously published protocol [16]. We used BioquantOsteo software to measure mineralizing surface per bone surface (MS/BS), mineral apposition rate (MAR) and bone formation rate per bone surface (BFR/BS).

Europe PMC Funders Author Manuscripts

Europe PMC Funders Author Manuscripts

Labeling interval for our study was 10 days. Tb. Rodent-VK blue TRAP F1 task list was used for MAR-BFR analysis. By using ROI cursor area of interest was drawn to determine BS and MS. Then by using specific preset for single labeling (l_4) and double labeling (l_5) area of interest was drawn and single labeled surface (sLS), double-labeled surface (dLS), inter-label thickness (IrLTh) were measured. Finally, BioquantOsteo software was used to calculate MAR and BFR by using the following formula; MAR = IrLTh/10 days (μm/day), BFR = MAR × (MS/BS) (μm/day) [16].

2.2.4 Serum PINP level determination—ELISA kits for rat pro-collagen type 1 N-terminal peptide (P1NP) were purchased from MyBioSource Inc. (San Diego, CA, USA) (Cat no. MBS775195). The experiment was performed as per manufacturer's protocol.

2.3 In vitro studies

2.3.1 Rat calvarial osteoblast culture and ALP assay—Osteoblasts were derived from calvarium of 1 to 2 day old rat pups as per our previously published protocol [14]. Cells at 90% confluence were trypsinized and seeded for experiments. Osteoblast differentiation was assessed by alkaline phosphatase (ALP) assay as per our previously published protocol [16]. Lira was used at six concentrations (10 pM, 100 pM, 1 nM, 10 nM, 100 nM, 1 μM) and vitamin D (10 nM) was used as positive control. Water was used as vehicle for Lira.

2.3.2 Osteoblast viability assay—Rat calvarial osteoblasts were cultured until 60% confluence and then treated with Lira (10 nM) for 48 h under serum deprived condition (1% FBS containing α -MEM) to induce loss of cell viability. 3-(4,5-dimethylthiazol-2-yl)-2,5-diphenyltetrazolium bromide (MTT) was added to the culture after 48 h treatment with Lira and incubated for 4 h at 37 °C. Dimethyl sulfoxide (DMSO) was added to solubilize the formazan crystal, formed by cellular metabolic activity. OD was measured at 570 nm.

2.3.3 Immunoblotting—Bone protein was isolated as described before [13]. Immunoblot analysis from bone and cultured cells were performed as described earlier [18] using indicated primary antibodies. Antibodies for immunoblotting were as follows: AMPKα (AMP-activated protein kinase; 1:1000, Cat no. 2532), pAMPKα (Thr172) (phosphorylated AMP-activated protein kinase, 1:1000, Cat no. 2531) and RunX2 (runt-related transcription factor 2, 1:1000, Cat no. 12556) from Cell Signaling Technologies (Danvers, MA, USA); AdipoR1 (Adiponectin receptor 1, 1:1000, Cat no. SC46748) from Santacruz (Dallas, TX, USA); GLP1R (Glucagon-like peptide-1 receptor, 1:1000, Cat no. 186051) from Abcam, PGC1α (Peroxisome proliferator-activated receptor gamma coactivator 1-alpha, 1:1000, Cat no. ST1208) from Calbiochem (Kenilworth, NJ, USA). All secondary antibodies were HRP conjugated (Sigma-Aldrich, St. Louis, MO, USA) and used at a final dilution of 1:5,000. We used HRP tagged β-actin from Sigma-Aldrich (1:25000, Cat no. A3854). Antibodies against succinate dehydrogenase complex, subunit A (SDHA), voltage-dependent anion channel 1 (VDAC1), and pyruvate dehydrogenase (PDH) were from Mitochondrial Sampler Kit (CST, Cat# #8674). Antibodies against cyochrome C oxidase subunit IV (COX IV, ab14744) and mitochondrial transcription factor A (TFAM, ab131607) were from Abcam (Cambridge, United Kingdom).

Europe PMC Funders Author Manuscripts

Europe PMC Funders Author Manuscripts

2.3.4 cAMP assay—Rat calvarial osteoblast was treated with Lira (10 nM) for 0 min, 5 min, 15 min, 30 min, 60 min and 90 min. After treatment, cAMP level in the lysate was determined by ELISA kit (Cayman Co., Ann Arbor, MI, USA) following the manufacturer's protocol. Total protein in each well was determined by BCA (Pierce, Rockford, IL, USA) to normalize cAMP data.

2.3.5 Glycolysis and mitochondrial respiration—Rat calvarial osteoblast was cultured in α -MEM with 10% FBS. 48 h prior to assay 40,000 cells/well were plated in a 24-well polystyrene Seahorse V7-PS Flux plate with no additional coating and treated with Lira (10 nM). Before starting the assay, cells were washed twice with assay media (XF Base minimal DMEM, Cat no 98546008) (Agilent Technologies, Santa Clara, CA, USA) and kept at 37 °C for 1 h. Glycolysis was analyzed by stepwise addition of A: glucose (10 mM), B: oligomycin (1 μM) and C: 2-deoxy-D-glucose (2-DG, 50 mM). Mitochondrial respiration was assayed by stepwise addition of A: oligomycin (1 μM), B: carbonyl cyanide-4-(trifluoromethoxy) phenylhydrazone (FCCP) (2 μM) and C: rotenone (0.5 μM). Three measurement cycles of 2 min mix, 1 min wait, and 5 min measure were carried out after each addition. The protein concentration of each well was measured by the BCA method after the assay to normalize the reading [13].

2.3.6 Assessment of mitochondrial status—SYBR Green-based (Thermo Fisher Scientific, Waltham, MA) RT-PCR was used to quantify mitochondrial DNA copy number (mtDNA) from total DNA isolated (PureLink® Genomic DNA Mini Kit, Thermo Fisher Scientific, Waltham, MA, USA) from Lira treated (0.3 mg/kg, s.c., for 5 days) newborn pups calvarium according to the manufacturer's protocol; The primers are as follows Cytochrome *B*: Forward 5′-TGAC CTTCCCGCCCCATCCA-3′, Reverse 5′ AGCCGTAGTTTACGTCTCGGCA-3; β-actin: Forward 5′-AGCGACGCGGAGCCAATCA 3′, Reverse-5′-TGCGCCGCCGGGTTTTATAG-3′[13].

Mitochondrial mass was determined by using Mitotracker Deep Red [19]. Rat calvarial osteoblast was treated with Lira (10 nM) for 48 h. After that cells were incubated with MitoTracker dye (200 nM) for 30 mins at 37 °C in serum-free media. The stained cells were fixed with 10% neutral buffered formalin, and images were captured using a fluorescence microscope at excitation 644, emission 665.

2.3.7 Statistical analyses—Data were expressed as the mean ± standard error of the mean (SEM). Statistical differences among the different treatment groups were analyzed by one-way ANOVA followed by a post hoc Newman-Keuls multiple comparison tests of significance using GraphPad Prism 5. Statistical significance has been denoted as $*p < 0.05$, $**p < 0.01$ and $***p < 0.001$ compared to sham or as indicated in the figure legend. Data having two groups were assessed by *t*-test to evaluate the statistical significance.

3 Results

3.1 Osteoinduction by Lira in osteopenic rats at the site of the osteotomy

We assessed bone regeneration ability of Lira in a femur osteotomy model made in adult female rats. Lira at two doses (0.3 mg/kg and 0.6 mg/kg) or vehicle (water, control) was

Europe PMC Funders Author Manuscripts

Europe PMC Funders Author Manuscripts

administered. Calcein labeling at the osteotomy site showed that Lira increased mineral deposition over control at both doses. Bone volume at the callus (BV/TV) was also significantly increased by the drug (Fig. 1A).

Since 0.3 mg/kg dose was effective, we next tested whether Lira had a similar effect in osteopenic rats given that bone regeneration is impaired under osteopenic condition [20]. In aged OVX rats, osteopenia was first induced as evident from decreases in femur metaphyseal volumetric BMD (vBMD, $P < 0.01$) and BV/TV ($P < 0.001$) compared to pre-surgery (ovary intact) stage (Fig. 1B). Lira (0.3 mg/kg) or vehicle (water) was administered to OVX (osteopenic) rats and calcein labeling data showed that the drug increased mineral deposition at callus site by ~120% over the vehicle (Fig. 1C). BV/TV was also significantly increased in the Lira group compared with control (Fig. 1C).

3.2 Liraglutide completely restored osteopenia and effect was comparable with PTH

At femur metaphysis (trabecular bone) BMD, BMC, and BV/TV were comparable between the control, Lira and PTH groups (Fig. 2A). Femur diaphysis is comprised of cortical bones and both treatments restored BMD, BMC, and Cs.Th to the sham levels (Fig. 2B). At L5, Lira restored BMD, BMC and BV/TV to the sham levels however all three parameters were higher in PTH than the sham group (Fig. 2C).

Rats in the OVX + veh and PTH groups were > 30% heavier than the sham and Lira groups (Table 1). Because body weight has a positive effect on BMD [21], we compared BMI-normalized BMD at femur metaphysis, diaphysis and L5 vertebrae (Fig. 2A–C). BMI data is given in Table 1. Lira completely restored BMI-normalized BMD of femur metaphysis and L5 vertebra, however at femur metaphysis, PTH failed to reach the sham level (Fig. 2A, C). At femur diaphysis, the BMI-normalized BMD between OVX and PTH groups were comparable whereas in the Lira group it was significantly increased over both OVX and PTH groups although it failed to achieve the sham level (Fig. 2B).

We next measured bone biomechanical strength by performing a compression test (axial load-bearing capacity) on the load-bearing L5 vertebra. Lira completely restored peak load, stiffness and energy to failure to the levels of sham (Fig. 2D). Next, linear regression analysis was performed to assess relationships between bone mass (BMC) and bone strength (peak load), that serve as surrogate measures of bone quality. Significant positive relationships were observed for L5 peak load versus BMC for all four groups, with r^2 value = 0.6503 ± 0.025 (Fig. 2E). For these regressions, slopes were significantly steeper for the sham, Lira and PTH groups versus OVX, indicating greater L5 strength than that was expected from the bone mass.

3.3 Osteoanabolic effect of liraglutide was involved in the restoration of osteopenia

In rat calvarial osteoblast (RCO), Lira significantly increased ALP activity (a surrogate of osteoblast differentiation) (Fig. 3A). Consistent with this *in vitro* data, we observed that Lira increased P1NP (serum osteogenic marker) over the sham and P1NP values in the Lira group was comparable to the PTH group (Fig. 3B). Moreover, since enhanced osteoblast differentiation favors cell survival and resistance to apoptosis, we tested the effect of serum

Europe PMC Funders Author Manuscripts

Europe PMC Funders Author Manuscripts

(growth factor) deprivation (apoptosis stimulus) on RCO survival and found that Lira significantly protected RCOs from the apoptosis stimulus (data not shown).

Stimulation of femur periosteal bone formation as observed with daily PTH injections results in an increase in cortical thickness (Cs.Th) (Fig. 2B), which in turn is known to increase resistance to fracture [22]. We thus measured cortical bone formation rate at femur diaphysis. Periosteal (p) MS/BS (percentage of bone surface undergoing active formation), pMAR (indicating an average rate of osteoblast activity) and pBFR/BS were decreased in OVX group and Lira increased these to sham levels (Fig. 3C). At femur metaphysis, all parameters (MS/BS, MAR, and BFR/BS) were decreased in the OVX group and Lira restored these to the sham level (Fig. 3D).

3.4 GLP1R, AdipoR1, and PGC1α expressions were restored in osteopenic bones by liraglutide

GLP1R, AdipoR1, and PGC1α expressions were reduced in femurs (devoid of marrow) of OVX rats compared with sham. Lira significantly increased GLP1R levels compared to OVX although it failed to restore GLP1R expression to the sham level (Fig. 4). The OVX-induced fall in AdipoR1 and PGC1α expressions were however completely restored to sham level by Lira. PTH had no effect on any of these proteins (Fig. 4).

3.5 Liraglutide induced osteoblast differentiation by activating GLP1R-cAMP-p-AMPK-AdipoR1-PGC1α signaling

At the osteogenic concentration (10 nM), Lira time-dependently (beginning at 24 h) increased GLP1R levels in RCO. In addition, Lira increased AdipoR1 (beginning 48 h) and PGC1α·expressions (beginning 24 h) in osteoblasts (Fig. 5A). As expected, Lira rapidly increased intracellular cAMP levels in RCO (maximum rise at 30 min) (Fig. 5B). Lira had no effect on the expression of AdipoR2 (data not shown). Exendin-3 and H89 blocked the Lira-induced increases in AdipoR1 and PGC1α, thus indicating the involvements of GLP1R and its downstream PKA in these processes. Accordingly, exendin-3 or H89 blocked the Lira-induced osteoblast differentiation (Fig. 5C, D).

RCOs exposed to Lira resulted in a rapid increase in AMPK phosphorylation (maximum increase at 30 min) (Fig. 5E), and this effect was blocked by H89, thus suggesting that PKA activation was required for AMPK activation (Fig. 5F). On the other hand, dorsomorphin (compound C), an AMPK inhibitor did not block the Lira-induced cAMP rise in RCO (Fig. 5G). Next, compound C blocked the Lira-induced upregulation of AdipoR1 and PGC1α (Fig. 5H). Moreover, compound C blocked the Lira-induced osteoblast differentiation (Fig. 5I). These data suggested that Lira via GLP1R resulted in PKA-dependent AMPK activation, which in turn led to the activation of AdipoR1 and PGC1α.

3.6 Liraglutide enhanced osteoblast differentiation via enhancing mitochondrial activity

Activation by Lira of cellular energy sensor, AMPK and mitochondrial biogenesis factor, PGC1α prompted us to study the effect of the drug on the metabolic profiles of RCO. The change in the pH of the culture medium was plotted as ECAR and was used as a measure of glycolysis. Lira caused no change in ECAR compared to vehicle (data not shown). All

Europe PMC Funders Author Manuscripts

Europe PMC Funders Author Manuscripts

mitochondrial respiratory parameters including basal and maximum respiration, spare respiratory capacity and ATP production were significantly increased by Lira (Fig. 6A). We next stained live RCO for mitochondria by MitoTracker Red CMXRos. Lira treatment for 48 h robustly increased mitochondrial staining compared to vehicle (Fig. 6B). We further confirmed the induction of mitochondrial biogenesis by assessing the expression of several mitochondrial proteins and observed that Lira increased TFAM, COX IV, VDAC1, PDH and SDHA expression over the vehicle (Fig. 6C).

Next, we treated RCO with 2-DG (to block glycolysis) or rotenone (to block mitochondrial complex 1 protein) and found that only the latter blocked Lira-induced osteoblastic differentiation, thus suggesting that mitochondrial function was required for the osteogenic effect of Lira *in vitro* (Fig. 6D).

We next studied the effect of Lira on mitochondrial biogenesis *in vivo* using calvarium of newborn rat pups that consists of pre-osteoblasts and osteoblasts [13,23]. Pups were injected with Lira (0.3 mg/kg, s.c.) for 5 consecutive days and mitochondrial DNA copy number was measured in the calvarium (Fig. 6E). Compared to vehicle, DNA copy number in Lira group was ~3.0-fold increased. Also, Runx2, the key osteoblast transcription factor was significantly enhanced in the calvarium of Lira-treated rat pups compared to control (Fig. 6F).

4 Discussion

The current study expands our understanding of the nature of bone restoration by Lira and for the first time links the osteoanabolic effect of Lira with mitochondrial biogenesis. The evidence of bone anabolic effect of GLP1R agonists including Lira [24] and exendin-4 [25] in postmenopausal osteopenic rodent model without diabetes is rather anecdotal. *De novo* bone formation by GLP1R activation has not been authentically established, and, in particular not compared with PTH, the “gold standard” osteoanabolic therapy. We observed that *de novo* formation of new trabecular mineralizing surfaces throughout the proximal femur metaphysis was increased by Lira and commensurates with PTH. The resultant osteogenic effect of Lira completely restored trabecular bones at the femur and lumbar vertebra – the clinically relevant sites for osteoporotic fractures in postmenopausal women. Bone mass-strength relationships indicate bone quality and are usually linear in normal adult animals. Treatments that impair matrix quality could alter bone mass-strength relationships resulting in an unfavorable biomechanical state [26], however, the effect of GLP1R activation in this regard was unknown. We showed that Lira had positive linear relationships between bone mass and strength, suggesting that the addition of new bone maintained bone quality comparable to sham or PTH group. BMI is considered to relate positively to BMD [27] and inversely to the risk of osteoporotic fracture [28–30]. Intriguingly, the BMI-normalized BMD in the femur by Lira were higher than PTH, indicating Lira’s superiority over PTH. An explanation for higher BMI normalized BMD in Lira over PTH is cannot be offered but could relate in part to the differences in the mode of action between the two drugs- PTH is anabolic, whereas Lira is osteoanabolic as conclusively demonstrated here as well as anti-catabolic as reported in osteopenic diabetic rats [2].

Europe PMC Funders Author Manuscripts

Europe PMC Funders Author Manuscripts

Lira also enhanced bone regeneration at the fracture site in osteopenic rats, suggesting its osteoinductive effect under a condition known for reduced osteogenic activity. This effect suggests Lira's potential use in difficult-to-heal osteoporotic fractures and for which there is no drug available. The underlying mechanism involves upregulation of GLP1R that elicits downstream signaling to stimulate mitochondrial biogenesis and upregulation of mitochondrial respiration leading to enhanced osteoblast differentiation.

Lira has been shown to increase the expression of GLP1R in differentiated 3T3-L1 adipocyte causing inhibition of lipogenesis [31] and in pulmonary pneumocytes resulting in decreased surfactant proteins in diabetic rats [32]. However, its effect on GLP1R expression and response in bone cells has not been studied. Furthermore, GLP-1 has been shown to protect neuronal cells from advanced glycation end product-induced mitochondrial damage [33] and recover the mitochondrial response to glucose in damaged pancreatic β cells [34], in addition to increasing mitochondrial mass in rat insulinoma cells [9] which suggested a regulatory effect of GLP1R on cellular energetics. We observed that Lira significantly increased mitochondrial biogenesis in osteoblasts which involved upregulation of GLP1R and AdipoR1. PTH which signals via PTH1R belonging to the same family B of GPCR as GLP1R had no effect on OVX-induced downregulation of GLP1R and AdipoR1, suggesting different modes of action vis-à-vis osteogenic effect by these two drugs.

We recently showed that AdipoR1 level was reduced in bones of OVX rats, and the osteogenic effect of globular adiponectin was associated with restoration of AdipoR1 in osteoblasts by this adipokine [13]. It is notable that the effects on bones and BMI by Lira as observed in this study and by globular adiponectin reported previously [13] appear similar. Since Lira stimulates AdipoR1 expression, this could result in a heightened AdipoR1 signaling *in vivo* by the circulating adiponectin pool, thereby raising the possibility of the convergence of GLP1R signaling into AdipoR1 activation. In this regard, futures studies investigating the effect of Lira/other GLP1R agonists in AdipoR1 null mice would provide a definitive answer.

Activation of GLP1R in the diabetic setting is known to increase serum adiponectin [35,36] but its effect on AdipoR1 expression remained unknown. Here we show that Lira restored the OVX-mediated fall in AdipoR1 in bones through GLP1R-mediated signaling in osteoblasts. Downregulation of AdipoR1 in bones and other tissues could imply a state of adiponectin resistance which could serve as a trigger for insulin resistance, the incidence of which is increased in postmenopausal women with higher BMI [37,38]. In the line of this argument, a GLP-1 resistance in OVX rats can also be speculated. Concomitant restoration of OVX-mediated loss of GLP1R and AdipoR1 by Lira suggests that the drug acts to overcome the state of adiponectin/GLP-1 resistance in OVX bones to achieve its osteoanabolic effect.

Since AdipoR1 activation in osteoblasts resulted in the upregulation of PGC1α (the mitochondrial biogenesis factor) leading to its osteogenic effect, we speculated that Lira through upregulation of AdipoR1 could stimulate mitochondrial function in osteoblasts. Indeed, Lira via GLP1R stimulated AdipoR1 and PGC1α through PKA-mediated AMPK

Europe PMC Funders Author Manuscripts

Europe PMC Funders Author Manuscripts

activation. To the best of our knowledge, this is the first report showing mitochondrial activation by GLP1R leading to osteogenic response.

Energy regulation of osteoblast is an emerging area of research and consensus is somewhat lacking regarding the glycolytic versus OxPhos dependent ATP generation by the differentiating osteoblasts. One report suggests that as they mature, RCOs use more OxPhos as ATP source [39]. Yet another report showed a dual increase in glycolysis and OxPhos in early stages of differentiation, and more glycolysis-derived ATP production at the mineralization stage [40]. PTH has been reported to induce aerobic glycolysis (so-called Warburg effect) in osteoblasts [11]. In our case, however, treating RCOs with Lira in the presence of osteogenic medium for 48 h (i.e. undergoing early stages of differentiation) resulted in increased OxPhos-dependent ATP production with no change in glycolytic parameters. In addition, Lira upregulated SDHA, a complex II protein whose inactivation leads to impaired OxPhos [41]. Given that Lira upregulated SDHA, it is plausible that SDHA was one of the mediators of Lira's effect. Furthermore, as PDH links glycolysis to TCA cycle by increasing acetyl CoA production and PTH inhibits PDH by upregulating pyruvate dehydrogenase kinase 1 [42], our observation of upregulation of PDH by Lira suggests a mitochondrial shift of osteoblast respiration from glycolysis. Moreover, COX-IV that catalyzes the final step in mitochondrial electron transport chain [43] is upregulated by Lira further attests to its role in stimulating OxPhos in osteoblasts. These data also highlights that at the level of osteoblast bioenergetics, Lira acts differently from PTH.

In osteoblasts, Lira increased TFAM which is not only required for the transcription of several respiratory chain proteins but also for the maintenance of mtDNA [44,45]. We observed that Lira increased mtDNA in osteoblasts *in vivo* which could be mediated by the upregulation of TFAM. VDAC1 is a mitochondrial outer membrane protein and is a modulator of mitochondria-induced apoptosis [46], and its upregulation by Lira appears to mediate the anti-apoptotic effect of Lira in osteoblasts. Thus, increased mitochondrial biogenesis and mitochondrial function appear to play key roles in Lira-induced osteoanabolic effect. Fig. 7 depicts the schematic diagram summarizing the signaling events involved in the osteogenic effect of Lira.

We conclude that Lira has osteoanabolic effect in OVX rats which is comparable to the standard-of-care, PTH, and this effect is mediated by stimulating mitochondrial biogenesis which is different from PTH.

Acknowledgments

This work was supported by CSIR project ASTHI (Anabolic Skeletal Targets in Health and Illness, BSC0201). Rohit A. Sinha is a Wellcome Trust/DBT IA fellow (IA/I/16/2/502691). The authors are thankful for the technical assistance provided by Dr. Kavita Singh at the confocal facility of the Electron Microscopy Unit, Sophisticated Analytical Instrument Facility (SAIF), CSIR-CDRI, Lucknow.

Supporting grants

Council of Scientific and Industrial Research, Government of India.

Europe PMC Funders Author Manuscripts

Europe PMC Funders Author Manuscripts

References

[1]. Astrup A, Rossner S, Van Gaal L, Rissanen A, Niskanen L, Al Hakim M, Madsen J, Rasmussen MF, Lean ME. Effects of liraglutide in the treatment of obesity: a randomised, double-blind, placebo-controlled study. Lancet. 2009; 374(9701):1606–1616. [PubMed: 19853906]

[2]. Wen B, Zhao L, Zhao H, Wang X. Liraglutide exerts a bone-protective effect in ovariectomized rats with streptozotocin-induced diabetes by inhibiting osteoclastogenesis. Exp Ther Med. 2018; 15(6):5077–5083. [PubMed: 29805533]

[3]. Nuche-Berenguer B, Moreno P, Portal-Nunez S, Dapia S, Esbrit P, Villanueva-Penacarrillo ML. Exendin-4 exerts osteogenic actions in insulin-resistant and type 2 diabetic states. Regul Pept. 2010; 159(1-3):61–66. [PubMed: 19586609]

[4]. Yamada C, Yamada Y, Tsukiyama K, Yamada K, Udagawa N, Takahashi N, Tanaka K, Drucker DJ, Seino Y, Inagaki N. The murine glucagon-like peptide-1 receptor is essential for control of bone resorption. Endocrinology. 2008; 149(2):574–579. [PubMed: 18039776]

[5]. Pereira M, Jeyabalan J, Jorgensen CS, Hopkinson M, Al-Jazzar A, Roux JP, Chavassieux P, Orriss IR, Cleasby ME, Chenu C. Chronic administration of Glucagon-like peptide-1 receptor agonists improves trabecular bone mass and architecture in ovariectomised mice. Bone. 2015; 81:459–467. [PubMed: 26314515]

[6]. Meng J, Ma X, Wang N, Jia M, Bi L, Wang Y, Li M, Zhang H, Xue X, Hou Z, Zhou Y, et al. Activation of GLP-1 receptor promotes bone marrow stromal cell osteogenic differentiation through beta-catenin. Stem Cell Rep. 2016; 6(4):579–591.

[7]. Lowell BB, Shulman GI. Mitochondrial dysfunction and type 2 diabetes. Science. 2005; 307(5708):384–387. [PubMed: 15662004]

[8]. Kwak SH, Park KS, Lee KU, Lee HK. Mitochondrial metabolism and diabetes. J DiabetesInvestig. 2010; 1(5):161–169.

[9]. Kang MY, Oh TJ, Cho YM. Glucagon-Like Peptide-1 Increases Mitochondrial Biogenesis and Function in INS-1 Rat Insulinoma Cells. Endocrinol Metab (Seoul). 2015; 30(2):216–220. [PubMed: 26194081]

[10]. Xu F, Lin B, Zheng X, Chen Z, Cao H, Xu H, Liang H, Weng J. GLP-1 receptor agonist promotes brown remodelling in mouse white adipose tissue through SIRT1. Diabetologia. 2016; 59(5):1059–1069. [PubMed: 26924394]

[11]. Esen E, Lee SY, Wice BM, Long F. PTH promotes bone anabolism by stimulating aerobic glycolysis via IGF signaling. J Bone Miner Res. 2015; 30(11):2137. [PubMed: 26477607]

[12]. Karner CM, Esen E, Okunade AL, Patterson BW, Long F. Increased glutamine catabolism mediates bone anabolism in response to WNT signaling. J Clin Invest. 2015; 125(2):551–562. [PubMed: 25562323]

[13]. China SP, Pal S, Chattopadhyay S, Porwal K, Kushwaha S, Bhattacharyya S, Mittal M, Gurjar AA, Barbhuyan T, Singh AK, Trivedi AK, et al. Chattopadhyay, Globular adiponectin reverses osteo-sarcopenia and altered body composition in ovariectomized rats. Bone. 2017; 105:75–86. [PubMed: 28811200]

[14]. Tripathi JK, Pal S, Awasthi B, Kumar A, Tandon A, Mitra K, Chattopadhyay N, Ghosh JK. Variants of self-assembling peptide, KLD-12 that show both rapid fracture healing and antimicrobial properties. Biomaterials. 2015; 56:92–103. [PubMed: 25934283]

[15]. Sharan K, Mishra JS, Swarnkar G, Siddiqui JA, Khan K, Kumari R, Rawat P, Maurya R, Sanyal S, Chattopadhyay N. A novel quercetin analogue from a medicinal plant promotes peak bone mass achievement and bone healing after injury and exerts an anabolic effect on osteoporotic bone: the role of aryl hydrocarbon receptor as a mediator of osteogenic action. J Bone Miner Res. 2011; 26(9):2096–2111. [PubMed: 21638315]

[16]. Pal S, Khan K, China SP, Mittal M, Porwal K, Shrivastava R, Taneja I, Hossain Z, Mandalapu D, Gayen JR, Wahajuddin M, et al. Chattopadhyay, Theophylline, a methylxanthine drug induces osteopenia and alters calciotropic hormones, and prophylactic vitamin D treatment protects against these changes in rats. Toxicol Appl Pharmacol. 2016; 295:12–25. [PubMed: 26851681]

[17]. Porwal K, Pal S, Dev K, China SP, Kumar Y, Singh C, Barbhuyan T, Sinha N, Sanyal S, Trivedi AK, Maurya R, et al. Guava fruit extract and its triterpene constituents have osteoanabolic effect:

Europe PMC Funders Author Manuscripts

Stimulation of osteoblast differentiation by activation of mitochondrial respiration via the Wnt/beta-catenin signaling. J Nutr Biochem. 2017; 44:22–34. [PubMed: 28343085]

[18]. Singh AK, Shree S, Chattopadhyay S, Kumar S, Gurjar A, Kushwaha S, Kumar H, Trivedi AK, Chattopadhyay N, Maurya R, Ramachandran R, et al. Small molecule adiponectin receptor agonist GTDF protects against skeletal muscle atrophy. Mol CellEndocrinol. 2017; 439:273–285.

[19]. Cottet-Rousselle C, Ronot X, Leverve X, Mayol JF. Cytometric assessment of mitochondria using fluorescent probes. Cytometry A. 2011; 79(6):405–425. [PubMed: 21595013]

[20]. Hak DJ. The biology of fracture healing in osteoporosis and in the presence of anti-osteoporotic drugs. Injury. 2018; 49(8):1461–1465. [PubMed: 29709376]

[21]. Salamat MR, Salamat AH, Janghorbani M. Association between obesity and bone mineral density by gender and menopausal status. Endocrinol Metab (Seoul). 2016; 31(4):547–558. [PubMed: 27834082]

[22]. Carpenter RD, Sigurdsson S, Zhao S, Lu Y, Eiriksdottir G, Sigurdsson G, Jonsson BY, Prevrhal S, Harris TB, Siggeirsdottir K, Guethnason V, et al. Effects of age and sex on the strength and cortical thickness of the femoral neck. Bone. 2011; 48(4):741–747. [PubMed: 21168538]

[23]. Nefussi JR, Brami G, Modrowski D, Oboeuf M, Forest N. Sequential expression of bone matrix proteins during rat calvaria osteoblast differentiation and bone nodule formation in vitro. J Histochem Cytochem. 1997; 45(4):493–503. [PubMed: 9111228]

[24]. Lu N, Sun H, Yu J, Wang X, Liu D, Zhao L, Sun L, Zhao H, Tao B, Liu J. Glucagon-like peptide-1 receptor agonist Liraglutide has anabolic bone effects in ovariectomized rats without diabetes. PLoS One. 2015; 10(7):e0132744. [PubMed: 26177280]

[25]. Ma X, Meng J, Jia M, Bi L, Zhou Y, Wang Y, Hu J, He G, Luo X. Exendin-4, a glucagon-like peptide-1 receptor agonist, prevents osteopenia by promoting bone formation and suppressing bone resorption in aged ovariectomized rats. J Bone Miner Res. 2013; 28(7):641–1652.

[26]. Hernandez CJ, Keaveny TM. A biomechanical perspective on bone quality. Bone. 2006; 39(6):1173–1181. [PubMed: 16876493]

[27]. Salamat MR, Salamat AH, Abedi I, Janghorbani M. Relationship between Weight, Body Mass Index, and Bone Mineral Density in Men Referred for Dual-Energy X-Ray Absorptiometry Scan in Isfahan, Iran. J Osteoporos. 2013; 2013

[28]. Soldin SJ, Hill JG. A rapid micromethod for measuring theophylline in serum by reverse-phase high-performance liquid chromatography. Clin Biochem. 1977; 10(2):74–77. [PubMed: 862179]

[29]. Porthouse J, Birks YF, Torgerson DJ, Cockayne S, Puffer S, Watt I. Risk factors for fracture in a UK population: a prospective cohort study. QJM. 2004; 97(9):569–574. [PubMed: 15317925]

[30]. Premaor MO, Pilbrow L, Tonkin C, Parker RA, Compston J. Obesity and fractures in postmenopausal women. J Bone Miner Res. 2010; 25(2):292–297. [PubMed: 19821769]

[31]. Chen J, Zhao H, Ma X, Zhang Y, Lu S, Wang Y, Zong C, Qin D, Yingfeng Yang Y, Wang X, Liu Y. GLP-1/GLP-1R signaling in regulation of adipocyte differentiation and lipogenesis. Cell Physiol Biochem. 2017; 42(3):1165–1176. [PubMed: 28668964]

[32]. Romani-Perez M, Outeirino-Iglesias V, Moya CM, Santisteban P, Gonzalez-Matias LC, Vigo E, Mallo F. Activation of the GLP-1 Receptor by Liraglutide Increases ACE2 Expression, Reversing Right Ventricle Hypertrophy, and Improving the Production of SP-A and SP-B in the Lungs of Type 1 Diabetes Rats. Endocrinology. 2015; 156(10):3559–3569. [PubMed: 26196539]

[33]. An FM, Chen S, Xu Z, Yin L, Wang Y, Liu AR, Yao WB, Gao XD. Glucagon-like peptide-1 regulates mitochondrial biogenesis and tau phosphorylation against advanced glycation end product-induced neuronal insult: Studies in vivo and in vitro. Neuroscience. 2015; 300:75–84. [PubMed: 25987199]

[34]. Ogata M, Iwasaki N, Ide R, Takizawa M, Uchigata Y. GLP-1-related proteins attenuate the effects of mitochondrial membrane damage in pancreatic beta cells. Biochem Biophys Res Commun. 2014; 447(1):133–138. [PubMed: 24709081]

[35]. Wang A, Li T, An P, Yan W, Zheng H, Wang B, Mu Y. Exendin-4 Upregulates Adiponectin Level in Adipocytes via Sirt1/Foxo-1 Signaling Pathway. PLoS One. 2017; 12(1):e0169469. [PubMed: 28122026]

Europe PMC Funders Author Manuscripts

[36]. Li D, Xu X, Zhang Y, Zhu J, Ye L, Lee KO, Ma J. Liraglutide treatment causes upregulation of adiponectin and downregulation of resistin in Chinese type 2 diabetes. Diabetes Res Clin Pract. 2015; 110(2):224–228. [PubMed: 26376464]

[37]. Varri M, Niskanen L, Tuomainen T, Honkanen R, Kroger H, Tuppurainen MT. Association of adipokines and estradiol with bone and carotid calcifications in postmenopausal women. Climacteric. 2016; 19(2):204–211. [PubMed: 26849745]

[38]. Chu MC, Cosper P, Orio F, Carmina E, Lobo RA. Insulin resistance in post-menopausal women with metabolic syndrome and the measurements of adiponectin, leptin, resistin, and ghrelin. Am J Obstet Gynecol. 2006; 194(1):100–104. [PubMed: 16389017]

[39]. Guntur AR, Le PT, Farber CR, Rosen CJ. Bioenergetics during calvarial osteoblast differentiation reflect strain differences in bone mass. Endocrinology. 2014; 155(5):1589–1595. [PubMed: 24437492]

[40]. Guntur AR, Gerencser AA, Le PT, DeMambro VE, Bornstein SA, Mookerjee SA, Maridas DE, Clemmons DE, Brand MD, Rosen CJ. Osteoblast-like MC3T3-E1 Cells Prefer Glycolysis for ATP Production but Adipocyte-like 3T3-L1 Cells Prefer Oxidative Phosphorylation. J Bone Miner Res. 2018; 33(6):1052–1065. [PubMed: 29342317]

[41]. Hwang MS, Rohlena J, Dong LF, Neuzil J, Grimm S. Powerhouse down: Complex II dissociation in the respiratory chain. Mitochondrion. 2014; 19(Pt A):20–28. [PubMed: 24933571]

[42]. Esen E, Lee SY, Wice BM, Long F. PTH promotes bone anabolism by stimulating aerobic glycolysis via igf signaling. J Bone Miner Res. 2015; 30(11):1959–1968. [PubMed: 25990470]

[43]. Li Y, Park JS, Deng JH, Bai Y. Cytochrome c oxidase subunit IV is essential for assembly and respiratory function of the enzyme complex. J Bioenerg Biomembr. 2006; 38(5-6):283–291. [PubMed: 17091399]

[44]. Bogenhagen DF, Rousseau D, Burke S. The layered structure of human mitochondrial DNA nucleoids. J Biol Chem. 2008; 283(6):3665–3675. [PubMed: 18063578]

[45]. Kukat C, Wurm CA, Spahr H, Falkenberg M, Larsson NG, Jakobs S. Super-resolution microscopy reveals that mammalian mitochondrial nucleoids have a uniform size and frequently contain a single copy of mtDNA. Proc Natl Acad Sci USA. 2011; 108(33):13534–13539. [PubMed: 21808029]

[46]. Reddy PH. Is the mitochondrial outermembrane protein VDAC1 therapeutic target for Alzheimer's disease? Biochim Biophys Acta. 2013; 1832(1):67–75. [PubMed: 22995655]

Europe PMC Funders Author Manuscripts

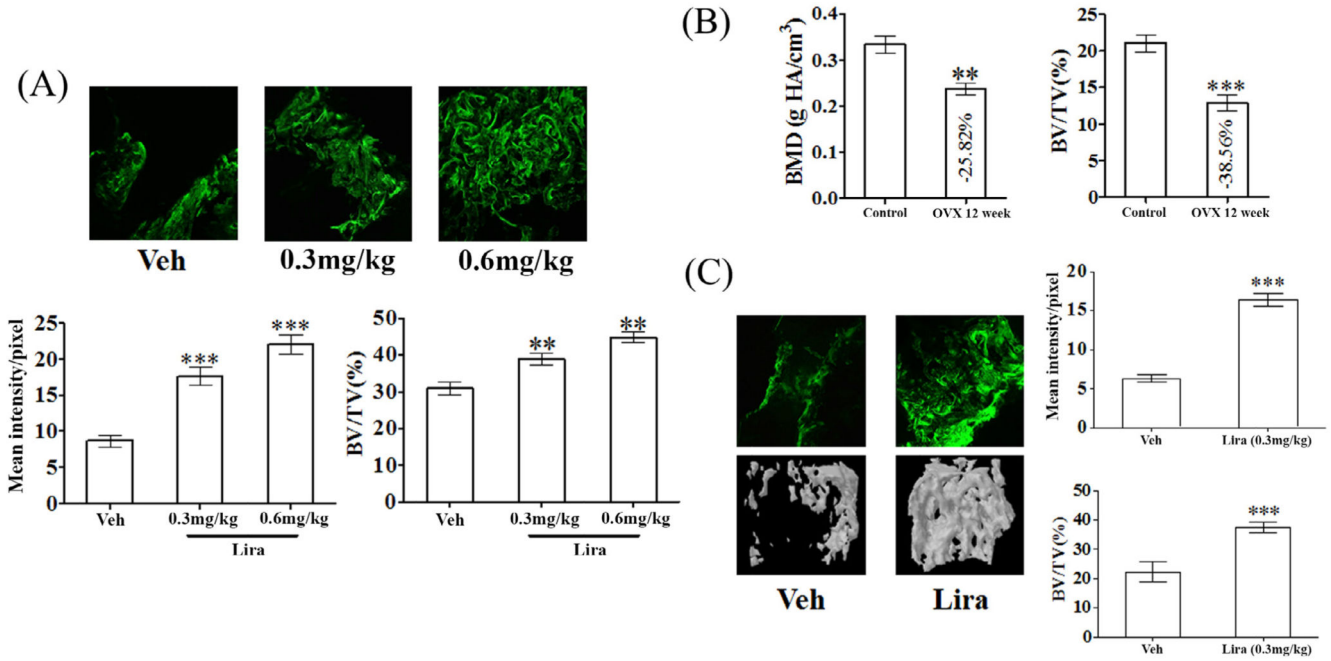

Fig. 1. Lira promotes osteoinduction and bone regeneration at the femur osteotomy site of normal and osteopenic rats.

(A) 24 h after making a 0.8 mm drill-hole at femur of adult female rats Lira treatment at indicated doses were given for 12 d. Representative confocal images (10×) showing calcein deposition in callus in various groups (upper panel). Quantification of mean calcein intensity per pixel in the callus is shown in the bottom panel. (B) Post-OVX induction of osteopenia in adult rats demonstrated by bone mineral density (BMD) and bone volume (BV/TV %) at proximal femur. (C) OVX osteopenic rats with drill-hole injury as described in panel A were treated with vehicle or Lira for 12 days. Shown are representative calcein labeling (upper left) and μCT images (bottom left) and quantification of mean calcein intensity and BV/TV (right panels). Data are expressed as mean ± SEM (n = 10/group); **P < 0.01 and ***P < 0.001 versus vehicle control.

Europe PMC Funders Author Manuscripts
Europe PMC Funders Author Manuscripts

Europe PMC Funders Author Manuscripts

Europe PMC Funders Author Manuscripts

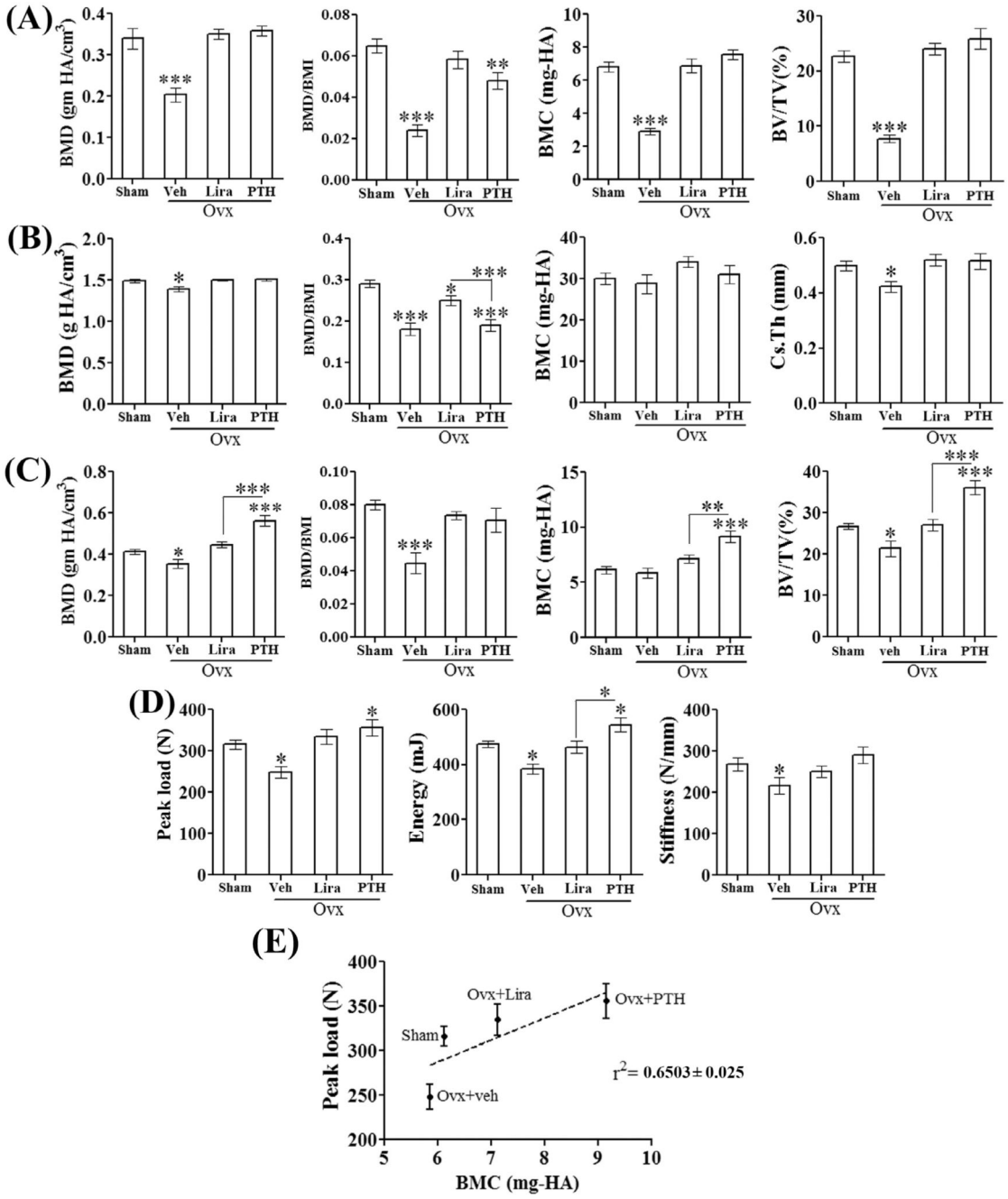

Fig. 2. Lira completely restored bone mass and strength in osteopenic rats.

Various parameters from (A) femur metaphysis (trabecular bone), (B) femur diaphysis (cortical bone) and (C) L5 vertebra (trabecular bone) are shown. (D) Destructive biomechanical testing data for L5 vertebra showing vertebral load bearing capacity and stiffness. (E) Linear regression analysis for L5 peak load versus BMC among different treatment groups, $r^2 = 0.6503 \pm 0.025$. Data are expressed as mean ± SEM (n = 8–10/group); *P < 0.05, **P < 0.01 and ***P < 0.001 versus sham.

Europe PMC Funders Author Manuscripts

Europe PMC Funders Author Manuscripts

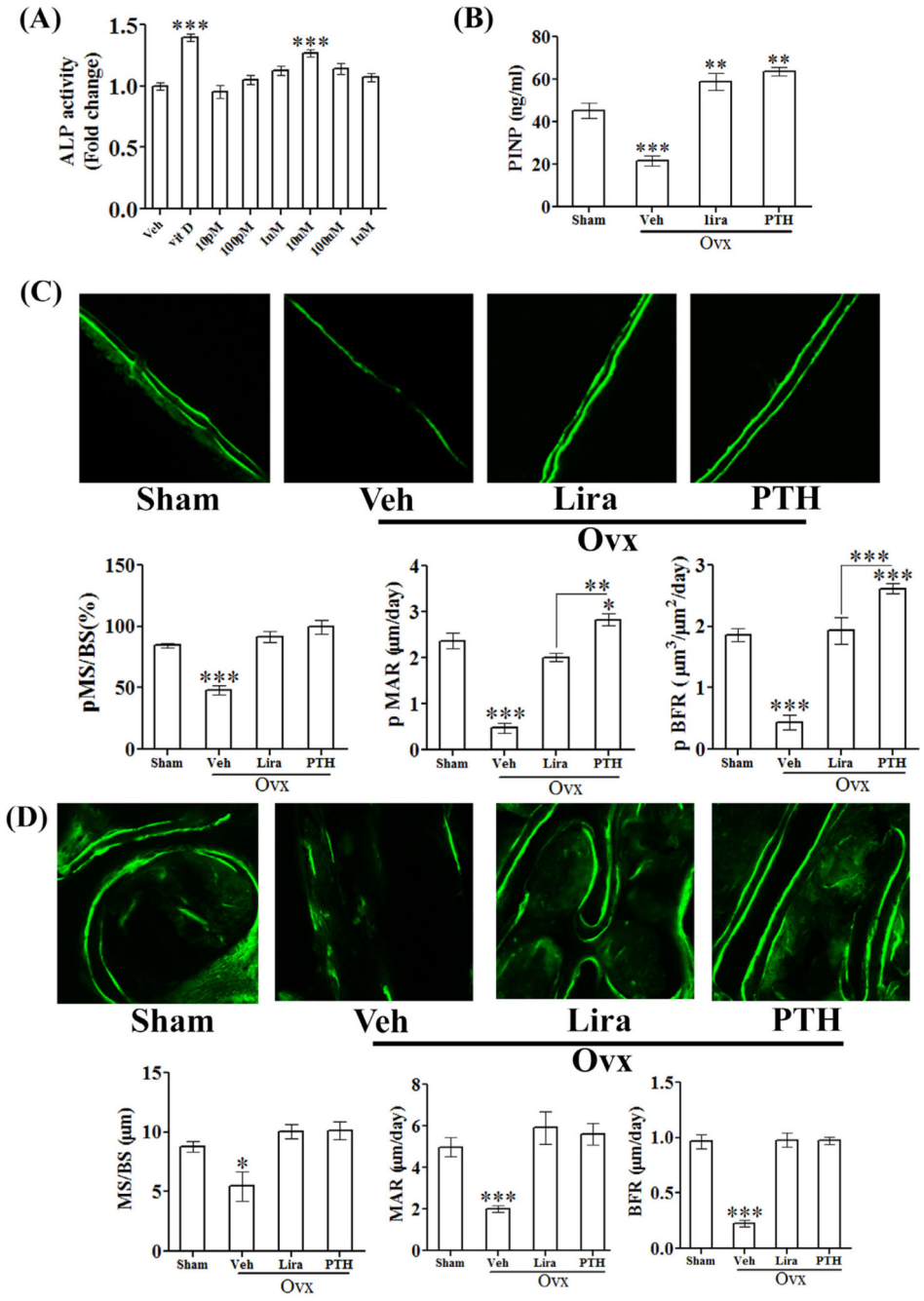

Fig. 3. Lira promoted bone formation in osteopenic rats.

(A) Differentiation of RCO was assessed by ALP assay. (B) The osteogenic marker, P1NP was assessed from the serum of indicated groups by ELISA. (C) Dynamic histomorphometry for femur diaphysis and (D) femur metaphysis. Data are expressed as mean ± SEM (n = 6/group); *P < 0.05, **P < 0.01 and ***P < 0.001 versus sham.

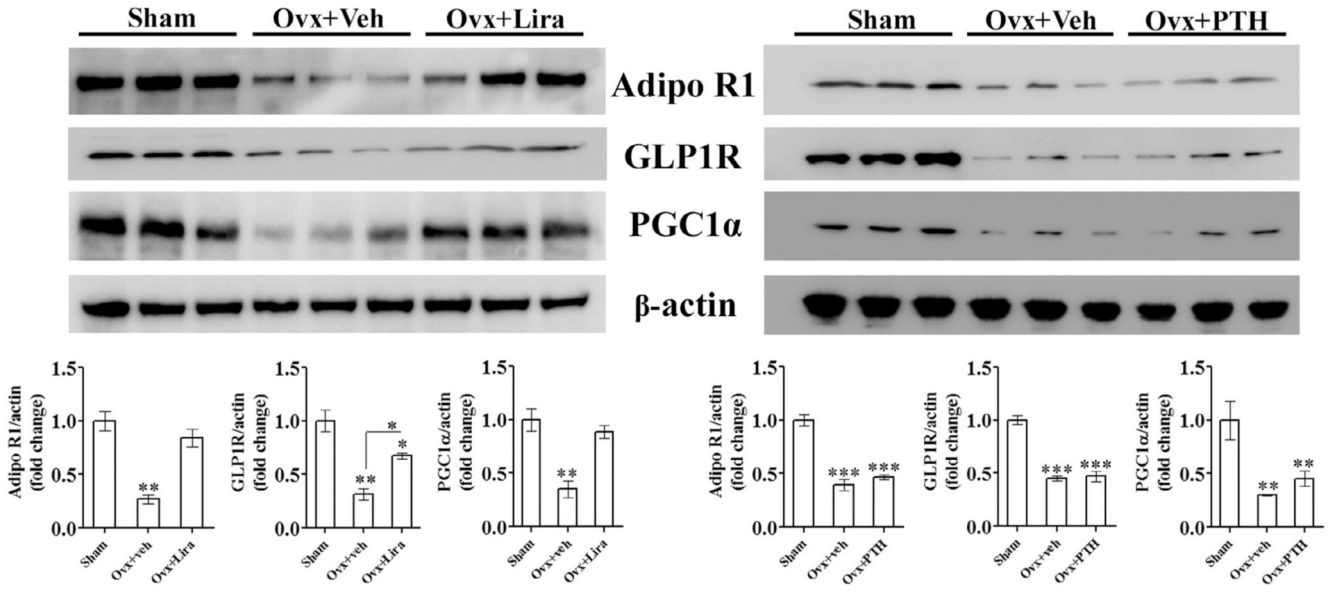

Fig. 4. Lira restored AdipoR1, GLP1R and PGC1α expression in osteopenic bones.

Immunoblots from femur proteins of indicated groups (upper panel) and densitometric data (lower panel) are shown. Data are expressed as mean ± SEM (n = 3/group); *P < 0.05, **P < 0.01 and ***P < 0.001 versus sham; and *P < 0.05 OVX + veh versus OVX + Lira.

Europe PMC Funders Author Manuscripts
Europe PMC Funders Author Manuscripts

Europe PMC Funders Author Manuscripts

Europe PMC Funders Author Manuscripts

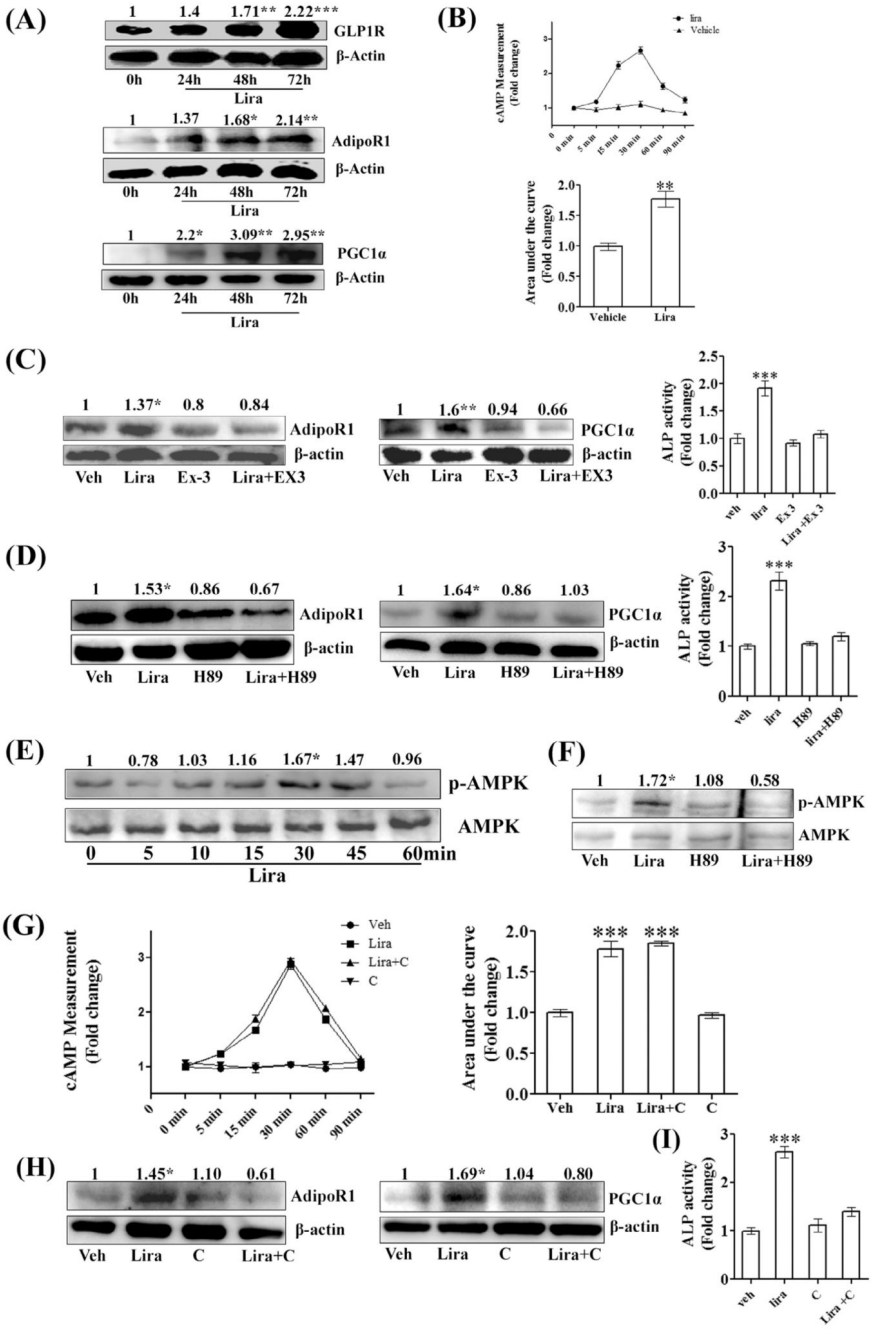

Fig. 5. Lira stimulated differentiation of RCO by activating GLP1R-cAMP-p-AMPK-AdipoR1-PGC1α signaling.

(A) Immunoblots showing upregulation of indicated proteins by Lira treatment (10 nM) at indicated time points along with densitometric values (in arbitrary unit). (B) Time-dependent rise in intracellular cAMP levels assessed by ELISA; the upper panel showing the temporal profile and the lower panel showing integral values (AUC). (C) Expression of AdipoR1 and PGC1α at 48 h assessed by immunoblotting with or without GLP1R inhibitor exendin-3 (Ex3, 1 μM). Bar diagram (right panel) showing RCO differentiation by ALP assay. (D) Expressions of AdipoR1 and PGC1α at 48 h assessed by immunoblotting with or without

PKA inhibitor H89 (1 μM). Bar diagram (right panel) showing RCO differentiation by ALP assay. (E) Phospho-AMPK (p-AMPK) time course assessment by immunoblotting. AMPK was used as loading control. (F) Expression of p-AMPK at 30 min assessed by immunoblotting with or without PKA inhibitor H89 (1 μM). (G) cAMP levels in RCO in presence of vehicle, Lira or Lira + dorsomorphin (compound C, 10 μM), an AMPK inhibitor. (H) Expression of AdipoR1 and PGC1α at 48 h assessed by immunoblotting; compound C (10 μM). (I) RCO differentiation is measured by ALP assay (48 h) at the indicated treatments. *P < 0.05, **P < 0.01, ***P < 0.001 compared with vehicle. All data are expressed as mean ± SEM from three independent experiments. In all experiments with inhibitors, RCO were pre-treated with inhibitors for 30 min.

Europe PMC Funders Author Manuscripts

Europe PMC Funders Author Manuscripts

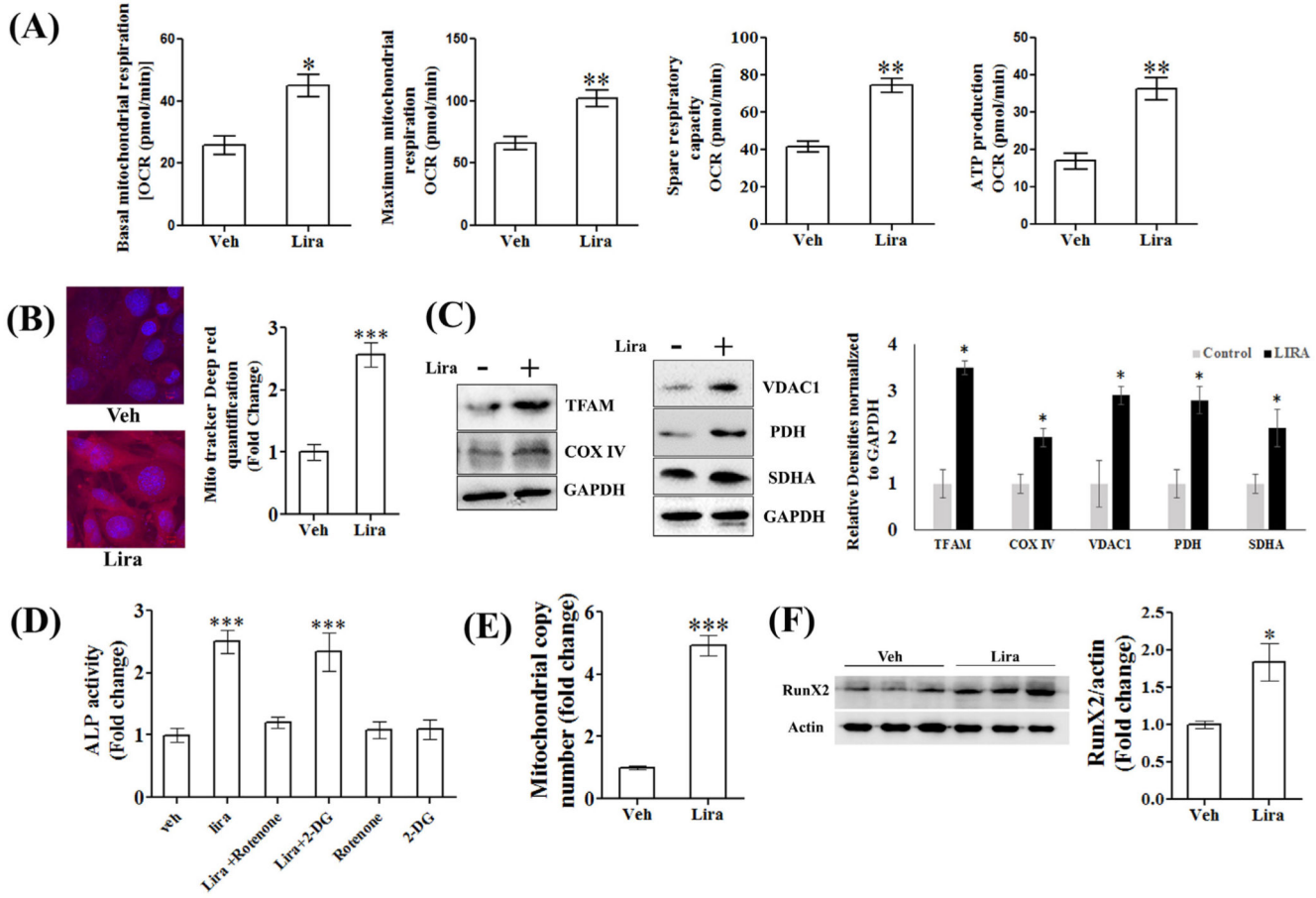

Fig. 6. Lira stimulated RCO differentiation by enhancing mitochondrial activity.

(A) Mitochondrial respiration in response to Lira (10 nM) was assayed by stepwise addition of i. 1 μM oligomycin, ii. 2 μM carbonyl cyanide-4-(trifluoromethoxy) phenylhydrazone (FCCP, a potent uncoupler of OxPhos) and iii. 0.5 μM rotenone (a blocker of complex 1 of mitochondrial electron transport chain), and basal mitochondrial respiration as oxygen consumption rate (OCR) was measured. Maximum mitochondrial respiration and ATP production were determined by treating cells with FCCP. Total protein was measured by the BCA method to normalize data. (B) Mito-tracker Deep red staining of RCO after 72 h Lira (10 nM) treatment; left panel, representative microscopy and right panel, quantification of fluorescent absorption. (C) Immunoblots showing upregulation of mitochondrial proteins by Lira treatment (10 nM) at 72 h and bar diagram showing densitometric quantification of bands in arbitrary unit. (D) RCO differentiation by ALP assay with indicated treatments; 0.5 μM rotenone, and 50 μM 2-DG, a glycolysis blocker. (E) Total DNA was extracted from calvarium of rat pups given indicated treatments and mitochondrial DNA copy number was determined by quantitative PCR. (F) Runx2 immunoblot from protein isolated from calvarium of rat pups given indicated treatments. *P < 0.05, **P < 0.01, ***P < 0.001 compared with vehicle. Data are expressed as mean ± SEM from three independent experiments. In all experiments with inhibitors, cells were pre-treated with inhibitors for 30

Europe PMC Funders Author Manuscripts
Europe PMC Funders Author Manuscripts

min. (For interpretation of the references to colour in this figure legend, the reader is referred to the web version of this article.)

Europe PMC Funders Author Manuscripts

Europe PMC Funders Author Manuscripts

Europe PMC Funders Author Manuscripts

Europe PMC Funders Author Manuscripts

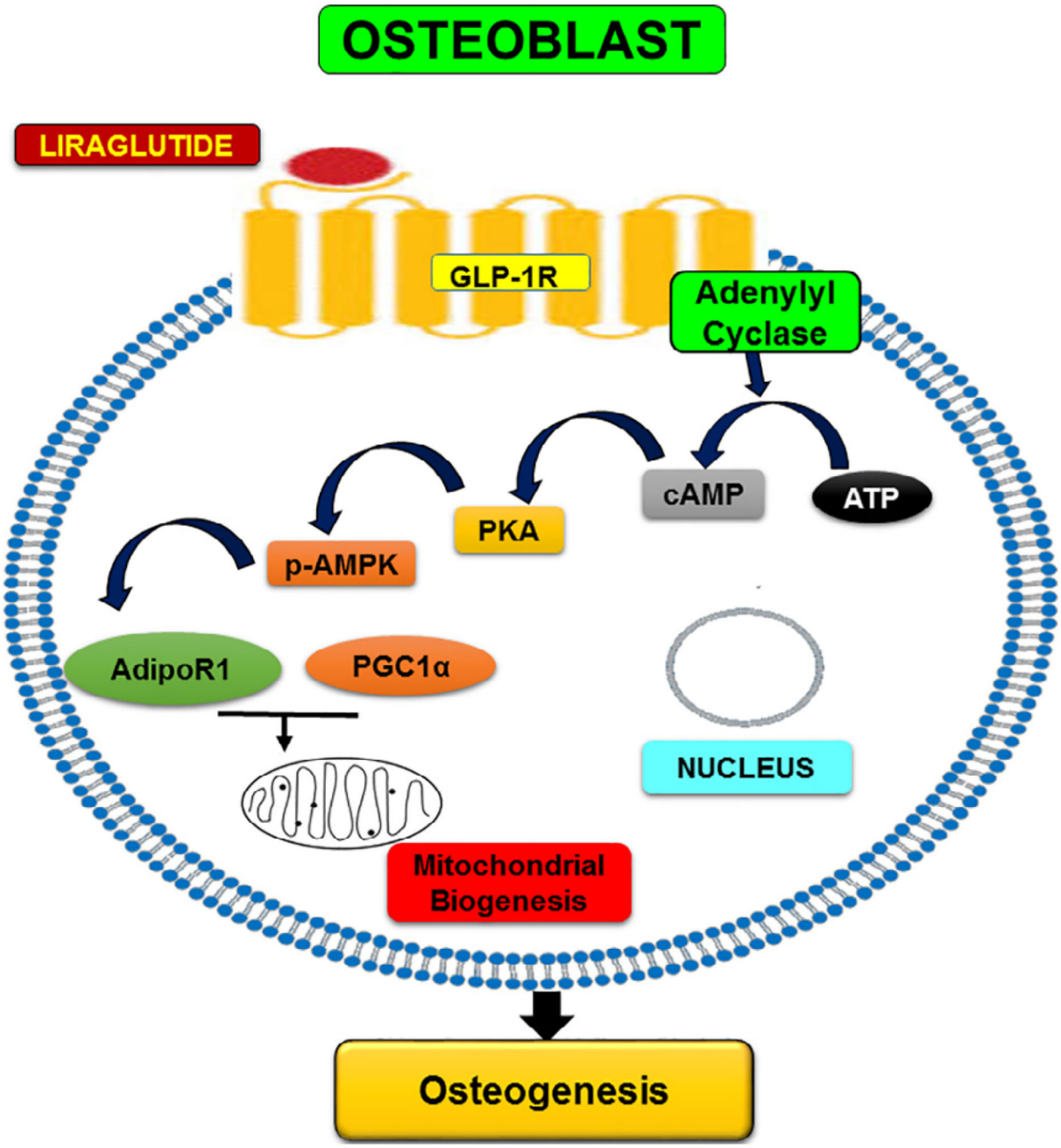

Fig. 7.
Schematic diagram showing Lira-induced signaling pathway resulting in osteogenesis.

Europe PMC Funders Author Manuscripts

Europe PMC Funders Author Manuscripts

Table 1

Body weight and BMI of different treatment groups.

	Sham	Ovx + Veh	Ovx + Lira	Ovx + PTH
Body weight (gm)	286.15 ± 8.39	420 ± 10.57***	304.2 ± 10.67	406 ± 6.48***
BMI	5.19 ± 0.17	8.10 ± 0.66***	6.11 ± 0.39	8.32 ± 0.63***

*** P < 0.001 compared with sham. Data are expressed as mean ± SEM (n = 6/group).